

Report

R-18-03

November 2018



Review of the Aaltonen-mechanism

Caitlin Huotilainen

Timo Saario

Aki Toivonen

SVENSK KÄRNBRÄNSLEHANTERING AB

SWEDISH NUCLEAR FUEL
AND WASTE MANAGEMENT CO

Box 3091, SE-169 03 Solna
Phone +46 8 459 84 00
skb.se

SVENSK KÄRNBRÄNSLEHANTERING

ISSN 1402-3091

SKB R-18-03

ID 1689627

November 2018

Review of the Aaltonen-mechanism

Caitlin Huutilainen, Timo Saario, Aki Toivonen
VTT Technical Research Centre of Finland Ltd

This report concerns a study which was conducted for Svensk Kärnbränslehantering AB (SKB). The conclusions and viewpoints presented in the report are those of the authors. SKB may draw modified conclusions, based on additional literature sources and/or expert opinions.

A pdf version of this document can be downloaded from www.skb.se.

© 2018 Svensk Kärnbränslehantering AB

Figure no	Credits
3-1	Permission requested.
3-2	Permission requested.
3-3	Permission requested.
3-4	Reprinted by permission from Springer Nature: Metallurgical and Materials Transactions A, Room-temperature diffusion in Cu/Ag thin-film couples caused by anodic dissolution, Denny A. Jones, Alan F. Jankowski, Gail A. Davidson, Copyright (1997).
3-5	Source of publication Taylor & Francis Ltd., Journal's web site: http://www.informaworld.com
3-6 left	Republished with permission of Electrochemical Society, Inc, from Radiation Induced Corrosion of Copper in Anoxic Aqueous, Å. Björkbacka, S. Hosseinpour, C. Leygraf and M. Jonssona, Copyright (2012); permission conveyed through Copyright Clearance Center, Inc.
3-6 right	Lousada, C. M. et al. Gamma radiation induces hydrogen absorption by copper in water. Sci. Rep. 6, 24234; doi: 10.1038/srep24234 (2016). https://creativecommons.org/licenses/by/4.0/
3-7 a, b	Lousada, C. M. et al. Gamma radiation induces hydrogen absorption by copper in water. Sci. Rep. 6, 24234; doi: 10.1038/srep24234 (2016). https://creativecommons.org/licenses/by/4.0/
3-8	Copyright © 2003 by The Minerals, Metals & Materials Society. Used with permission.
3-9	Permission requested.
3-10	Xing-Long Ye and Hai-Jun Jin, Electrochemical control of creep in nanoporous gold, Vol 103, Article ID 201912, 2013; licensed under a Creative Commons Attribution (CC BY) license.
3-11	Reprinted from Corrosion Science, Stress corrosion crack propagation in α -brass and copper exposed to sodium nitrite solutions, J. Yu, R.N. Parkins, Copyright (1987), with permission from Elsevier.

Preface

In this work the Aaltonen-mechanism of stress corrosion cracking, suggesting a critical role of vacancies in the metal, and its possible relevance to the stability of phosphorus micro-alloyed copper under repository conditions with sulphide, has been described and studied in response to the concerns expressed by the Radiation safety authority in Sweden, SSM, in their report 2018:07 and the Land and Environmental Court in Sweden, in their statement of Yttrande M 1333-11.

Contents

1	Introduction	7
2	Goal	9
3	Results	11
3.1	Aaltonen-mechanism	11
3.2	Studies on SCC of copper in sulphide containing water	12
3.3	Hydrogen in copper: corrosion, vacancy stabilization, γ -radiation and the Aaltonen-mechanism	14
3.4	Creep as an essential feature in the Aaltonen-mechanism; effect of anodic polarization on creep – results from literature	20
3.5	Corrosion rate vs current density	23
4	Conclusions	25
5	Summary	27
	References	29

1 Introduction

The Radiation safety authority in Sweden, SSM, in their report 2018:07 and the Land and Environmental Court in Sweden – in their statement of Yttrande M 1333-11, both express their concern about the possibility of the so-called Aaltonen mechanism in reference to the stress corrosion cracking of phosphorus micro-alloyed copper, CuOFP, in presence of sulphide in the repository environment.

Three scientific publications are specifically referred to by SSM and the Land and Environmental Court in Sweden in their statement (Aaltonen et al. 1998, 2003, Jagodzinski et al. 2000). The first publication, by Aaltonen et al. discusses the introduction of vacancies into CuOF when anodically polarised in 0.3 M sodium nitrite, NaNO₂, solution (Aaltonen et al. 1998), while the second publication, by Jagodzinski et al. discusses the same phenomena (in addition to CuOF) in admiralty brass exposed to hot tap water under anodic polarisation and an Al-5Mg-alloy exposed to 0.05 N KOH solution without anodic polarisation (Jagodzinski et al. 2000). The third publication, again by Aaltonen et al. discusses the electrochemical behaviour of Cu in 0.3 M NaNO₂ solution and tap water, as well as the effect of anodic polarisation in 0.3 M NaNO₂ solution on creep behaviour of Cu (Aaltonen et al. 2003).

A description of the so-called Aaltonen mechanism is given in this document, along with a review of available literature concerning the issues and questions brought up in the Yttrande M 1333-11 statement and SSM report 2018:07.

2 Goal

The goal of this work has been to assess the available information regarding the susceptibility of copper to stress corrosion cracking in sulphide containing water through the vacancy-creep mechanism, i.e. the so-called Aaltonen-mechanism. In addition, the possible role of hydrogen produced by the copper oxidation process in the said stress corrosion cracking mechanism was also assessed.

3 Results

3.1 Aaltonen-mechanism

Metallic materials always contain as a minimum a temperature dependent equilibrium concentration of metal vacancies (empty metal atom sites in the metal lattice), according to Equation 3-1.

$$N_v(T) = N \cdot \exp\left(\frac{-E_f}{kT}\right) \quad (\text{Equation 3-1})$$

where $N_v(T)$ = number of vacancies at temperature T , N = number of atomic sites in the lattice, E_f = vacancy formation energy, k = Boltzmann's constant (1.38×10^{-23} J/K or 8.62×10^{-5} eV/K) and T = temperature in Kelvin degrees. In case of copper, the vacancy formation energy has been reported to be 1.27 eV (Bourassa and Lengeler 1976). Thus, for example, the equilibrium concentration of vacancies in copper increases by about $\times 20.000$ when temperature increases from $T = 25$ °C to $T = 100$ °C.

In the Aaltonen-mechanism of stress corrosion cracking (SCC), first introduced in 1996 (Aaltonen et al. 1996) as a general model for metals, it is in principle proposed that an excessive surplus of metal vacancies in the metal lattice, forming as a consequence of metal dissolution, oxidation or reduction at the metal/electrolyte interface, concentrate within the metal to the extent enabling line dislocation sources¹ (such as the Bardeen-Herring source) to become activated. The Aaltonen-mechanism is explained schematically in Figure 3-1 (Aaltonen et al. 1996).

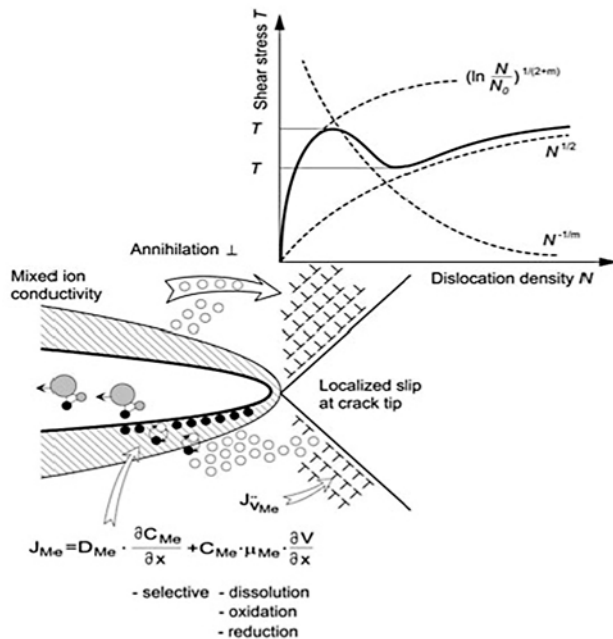


Figure 3-1. Principle of the Aaltonen-mechanism of SCC (Aaltonen et al. 1996). The flux of metal vacancies, $J_{v_{Me}}$, accelerated due to dissolution and oxidation (reduction) of metal at the metal-electrolyte-interface, becomes annihilated at dislocations ahead of the crack tip at the area of elevated shear stress, enabling dislocation multiplication, movement and climb, thus producing enhanced localised deformation (slip), resulting in breaking of the surface film and advancement of the crack.

¹ A line dislocation is an imperfection in the metal lattice that transmits deformation, e.g. slip, on a metal lattice plane; a Bardeen-Herring dislocation source can produce dislocations that can climb, not only move ahead on a single metal lattice plane. A dislocation source is for example two inclusions at the two ends of a dislocation. Under sufficient stress, a dislocation can break free of the inclusions and travel through the metal lattice, producing deformation (slip), while leaving behind a “mother” dislocation which can emit more dislocations, provided the stress remains high enough (Hirth and Lothe 1968).

The activation of dislocation sources then may lead to strain (slip) localisation at the crack tip, resulting in breaking of the surface film at the crack tip, exposing fresh metal surface. The fresh metal surface again oxidises in contact with the electrolyte resulting in forming a new surface film, further metal oxidation and dissolution and repetition of the phenomena, thus producing crack growth. In this respect, the Aaltonen-mechanism can be considered a further refinement of the generally accepted slip-oxidation mechanism (King and Newman 2010, Jones 1992) (explaining the enhancement of the slip-part in more detail), and not a separate SCC mechanism per se. A rather thorough discussion on the possibility of SCC in copper with the slip-oxidation mechanism has been presented by King and Newman (2010), and is thus not presented here.

Oxidation means that metal atoms from the lattice oxidise to positively charged metal ions, i.e. they donate electrons. The electron receiver can be e.g. dissolved oxygen in water (forming copper oxide), or dissolved sulphide in water (forming copper sulphide), or some other entity. Thus, oxidation of copper does occur also in the absence of oxygen, e.g. in the presence of sulphide, and thus, presumably, vacancies can form also when copper corrodes (oxidises) in sulphide containing water. However, to the knowledge of the authors of this report, no studies of vacancy formation as a result of copper corrosion (oxidation) in presence of sulphide have been conducted.

3.2 Studies on SCC of copper in sulphide containing water

Taniguchi and Kawasaki reported in 2008 that copper may be susceptible to stress corrosion cracking (SCC) in seawater with sulphide (Taniguchi and Kawasaki 2008). Their experiments were performed at $T = 80\text{ }^{\circ}\text{C}$ and with the slow strain rate technique (SSRT), in which a tensile specimen is slowly pulled into fracture while exposed to the environment. The maximum concentration of sulphide in their experiments was 10^{-2} M ($0.01\text{ mol/litre} = 330\text{ wt ppm}$). They found surface cracks extending for a few tens of micrometers from the surface and interpreted this as indicative of SCC. No examination of unexposed samples or areas of exposed samples outside the straining area was reported.

Ariilahti et al. (2011) performed tests with fracture mechanical specimens (1"CT-type), in which an artificial crack is introduced to the material by fatigue in air and then the specimen is exposed to the experimental environment and loaded to a pre-described level. In their tests in artificial groundwater at sulphide concentration of $6 \times 10^{-3}\text{ M}$, they found no indication of SCC. Their initial claim of possible in-diffusion of sulphide into CuOFP through grain boundaries, was later (Sipilä et al. 2014) assumed to be caused by surface diffusion of sulphide during the post-handling of the specimens, i.e. an experimental artefact.

Sipilä et al. (2014), in their study of CuOFP using slow strain rate tests (SSRT) in artificial groundwater with $6 \times 10^{-3}\text{ M}$ sulphide at room temperature (RT), found no evidence for SCC.

Bhaskaran et al. (2013), in their experiments with CuOFP and CuOFHC at temperatures of room temperature (RT) and $80\text{ }^{\circ}\text{C}$ and with sulphide concentrations varying between $5 \times 10^{-3}\text{ M}$ and $50 \times 10^{-3}\text{ M}$ and chloride (10^{-1} M), found no evidence for SCC.

In another SKB report by Taxén et al. (2018) no indication of SCC was found in CuOFP tested in 10^{-2} M sulphide containing water at temperatures of $T = \text{RT}$ and $80\text{ }^{\circ}\text{C}$.

Becker and Öijerholm (2017) presented SSRT-results of copper (CuOFP) in sulphide and chloride (10^{-1} M) containing water at $T = 90\text{ }^{\circ}\text{C}$ and tested up to about 9 % of strain. They claim to have found SCC at the highest sulphide concentration, 10^{-3} M , but not at the two lower concentrations of 10^{-4} M and 10^{-5} M . Their claim is based on the finding of surface defects that look like small initiated cracks. In their study, they found similar defects also inside the material and in non-deformed non-exposed areas, indicating that these defects have their origin in the manufacturing process. The depth of these defects is from a few microns to a few tens of microns, i.e. similar to the findings of Taniguchi and Kawasaki (2008). An alternative plausible explanation of their claimed finding of SCC at the highest sulphide concentration studied is that sulphide, as a surface active species, is able to diffuse into the defects (in case that they reach the surface) producing lowering of the cohesive forces (Lejček 2010) and thereby enabling opening up of the pre-existing defects under straining. The thus opened-up manufacturing defects would have the appearance of a surface crack, and could thus be erroneously interpreted as SCC.

Björkblad and Faleskog (2018) show that defects similar to those found by Becker and Öijerholm are also found in specimens tested under creep conditions at temperatures ranging from $T = 75\text{ °C}$ to 175 °C . i.e. with no contact to water but up to relatively high strains. This further corroborates the line of thinking that the defects interpreted by Becker and Öijerholm as SCC are indeed pre-existing manufacturing defects, opening up of which is accelerated by the presence of a high concentration of sulphide in the water.

In a paper by Forsström et al. (2017), three of the samples in the Becker and Öijerholm report (Becker and Öijerholm 2017) were further analysed for hydrogen concentration, Figure 3-2 (drawn based on the data shown by Forsström et al.). It is clear that the absorbed hydrogen concentration (about twice as high as in the original unexposed CuOFP material, $\approx 0.5\text{ wt ppm}$) has no correlation with the sulphide concentration in the water. This may be taken as indicative that the absorbed hydrogen has no correlation with the opening up of the surface defects, claimed to be SCC by Becker and Öijerholm. Forsström et al. (2017) also studied the surface defects using Electron back-scattered diffraction (EBSD), showing evidence for very little plastic deformation along the assumed crack path. This could be taken as an indication of the defect growth during exposure or, alternatively, that the defects originate from manufacturing as initially relatively sharp and do not grow due to the exposure. The nature of the similar internal defects, that had never been in contact with the sulphide containing environment, was unfortunately not further examined. The hypothesis (Forsström et al. 2017) that the internal defects (described as chain of voids) are caused by hydrogen uptake and in-diffusion is unlikely, since similar amounts of hydrogen were found in all locations of the samples (irrespective of the sulphide concentration of the environment), also the part used to fasten the samples in the loading machine.

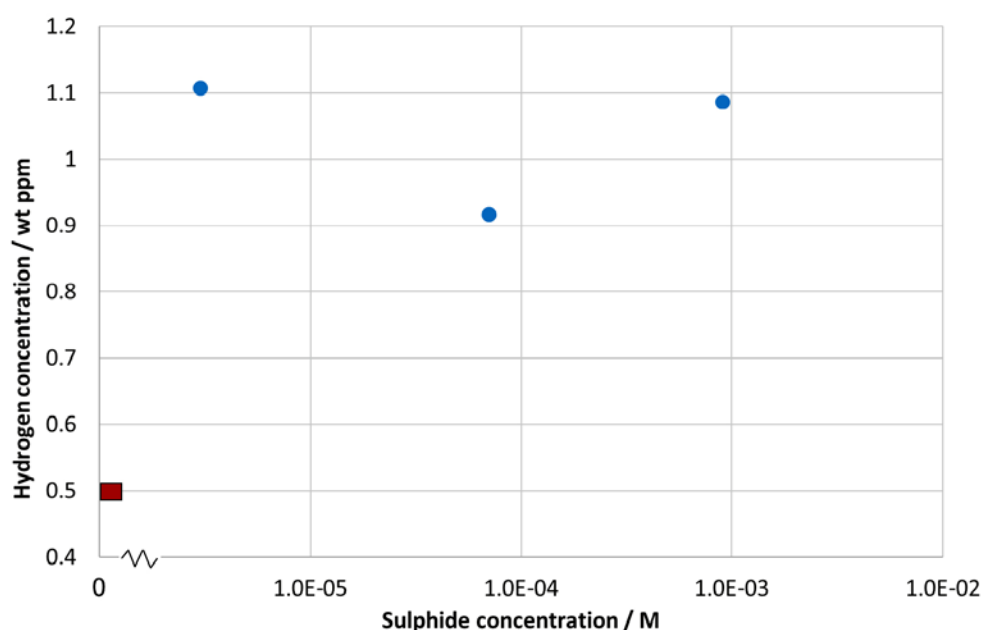


Figure 3-2. Hydrogen concentration of CuOFP in original material (red bar, average of two measurements) and after two week exposure to water with chloride (10^{-1} M) at $T = 90\text{ °C}$ with three different sulphide concentrations (blue circles, average of several measurements), tested up to 9 % strain in slow strain rate tests, drawn with data from Forsström et al. (2017).

3.3 Hydrogen in copper: corrosion, vacancy stabilization, γ -radiation and the Aaltonen-mechanism

The possible generation of hydrogen in corrosion processes needs also to be considered in the discussion of mechanical properties of copper in a repository environment. Although in a pure water environment, copper and its protective oxides can be thermodynamically stable, their stability significantly decreases in the presence of chloride and/or sulphide ions. The corrosion reaction in the presence of these ions creates a hydrogen source. Some of this hydrogen produced will be absorbed by the copper. After entering the metal, hydrogen will be transported across the canister via interstitial diffusion processes. The hydrogen atoms will interact with both interstitial lattice sites and the intrinsic metallurgical heterogeneities present in the material, e.g. dislocations, impurity atoms (such as S, P, O, Ni, etc), vacancies, di-vacancies and vacancy clusters, etc. Hydrogen uptake over time, and its possible accumulation, or trapping, at metallurgical heterogeneities, could have an effect on the canister's long-term mechanical properties, including ductility, toughness, creep properties, and [sulphide] SCC resistance/behaviour.

The Aaltonen-mechanism, i.e. a refined slip-oxidation SCC mechanism, could be considered to be affected and/or enhanced in the presence of hydrogen. It can be considered that the H content of "pure" copper is dependent on the level of oxygen present in the material and the solubility of hydrogen, and its isotopes is highly dependent on the oxygen content of copper, as shown in Figure 3-3 for different types of copper (Caskey et al. 1975). While hydrogen is considered to have

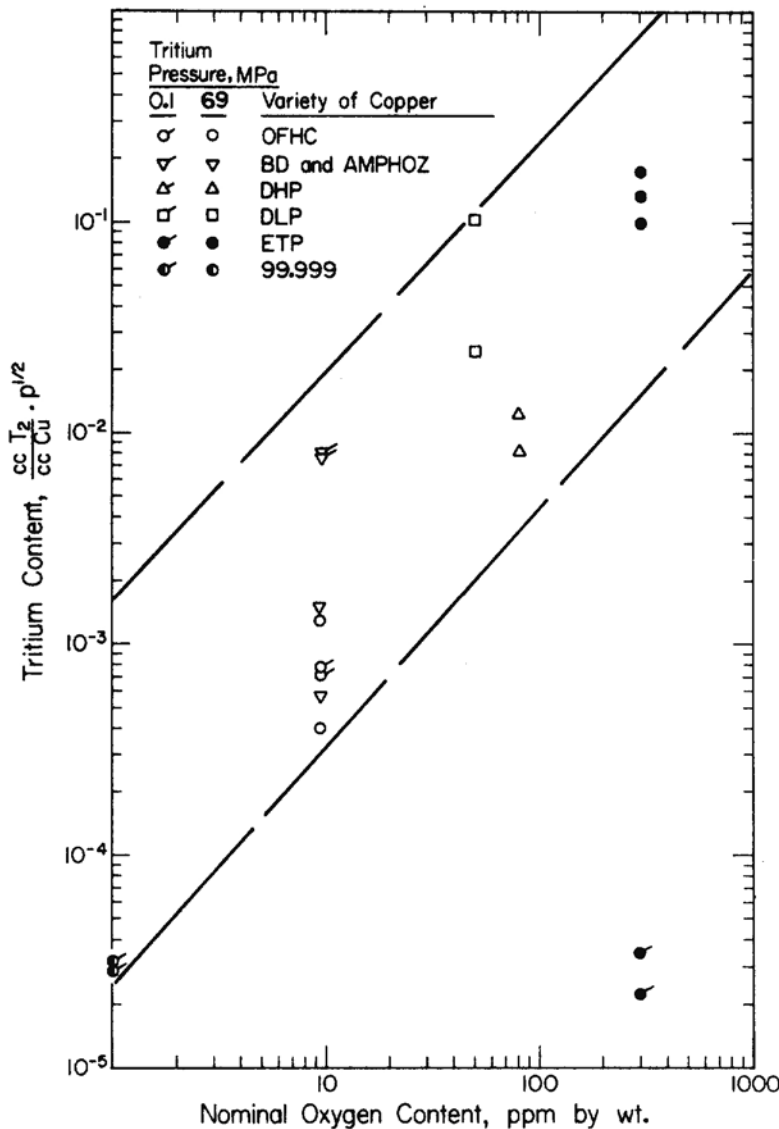


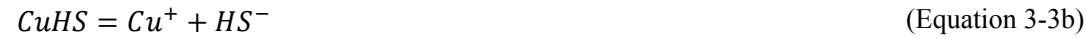
Figure 3-3. Absorbed tritium (^3H , isotopic tracer of hydrogen) versus oxygen content for copper (from Caskey et al. 1975).

a very small effect on the mechanical behaviour of pure copper² (San March and Somerday 2012), a small amount of oxygen can cause a significant increase in its sensitivity. The increased sensitivity is due to the formation of micro-voids, preferentially located along the grain boundaries, filled with high fugacity water vapour, possibly as a result of cuprous oxide reduction by hydrogen, which has been proposed to possibly lead to the hydrogen embrittlement of the alloy (Mattsson and Schueckher 1958). However, since the oxygen concentration in CuOFP is less than 5 ppm, the effect of oxygen on hydrogen concentration (according to Figure 3-3) can be considered to be insignificant.

As previously mentioned, vacancies are inherently present in materials, at least at their equilibrium concentration. An excess of vacancies can be produced e.g. via oxidation (i.e. corrosion). During the corrosion process of copper in sulphide containing environment, an excess of vacancies are generated³ and hydrogen is produced via the general oxidation reaction, where the cathodic reaction can be expressed by:



and the anodic reaction expressed by:



The hydrogen sulphide ion can produce hydrogen at the copper surface by:



A portion of the generated hydrogen (H_{ads}) can be absorbed by the Cu metal and then diffuse across the material as H atoms, and possibly form hydrogen gas in the microvoids present in the material.

Evidence for the long-range vacancy diffusion is provided by the work of Jones et al. (1997). They studied the effects of anodic polarization on bimetallic Cu/Ag films (100 nm film of Cu was sputtered on top of a 100 nm film of Ag that was first sputtered on a Si-wafer). The specimens were immersed in 0.5 M H_2SO_4 solution and polarized to anodic direction with current densities of 0.056–0.900 mA/cm². After the exposure, the concentration profiles of Cu, Ag and oxygen were measured using argon sputtering and simultaneous Auger Electron Spectroscopy (AES) measurement. They observed evolution of concentration profiles (Kirkendall-type interface movements) at the Cu-Ag interface as a function of polarization time and current in the polarized specimens. They concluded that the effect resulted from diffusion of vacancies (as di-vacancies) generated by anodic dissolution of Cu from the surface to the interface. This was not seen in non-polarized reference specimens. The diffusivities they estimated from the data of the polarized samples were very high, i.e. $\sim 10^{-12}$ cm²/s for Ag in Cu, as compared to what is generally accepted for room temperature grain boundary (GB) diffusion values extrapolated from data in Figure 4-2 in Magnusson and Frisk (2013) ($< 10^{-15}$ cm²/s for Cu in Cu and $< 10^{-18}$ cm²/s for Ag in Cu). The data of Jones et al. (1997) is shown in Figure 3-4. Further evidence of vacancy generation on the polarized surface and their diffusion to the Cu-Ag interface was interface voids observed by TEM.

² In its non-hydrogen saturated condition. The availability of mechanical testing data for hydrogen-saturated pure copper is limited according to Forsström et al. (2017).

³ The volume of copper(I) sulphide to that of copper metal is about 2.0. Thus, for each copper atom consumed in forming the sulphide, one additional copper atom has to be transferred from the metal lattice (by diffusion through the sulphide), leaving an empty metal atom site (vacancy) behind, to the oxide/water interface where the copper atom is dissolved.

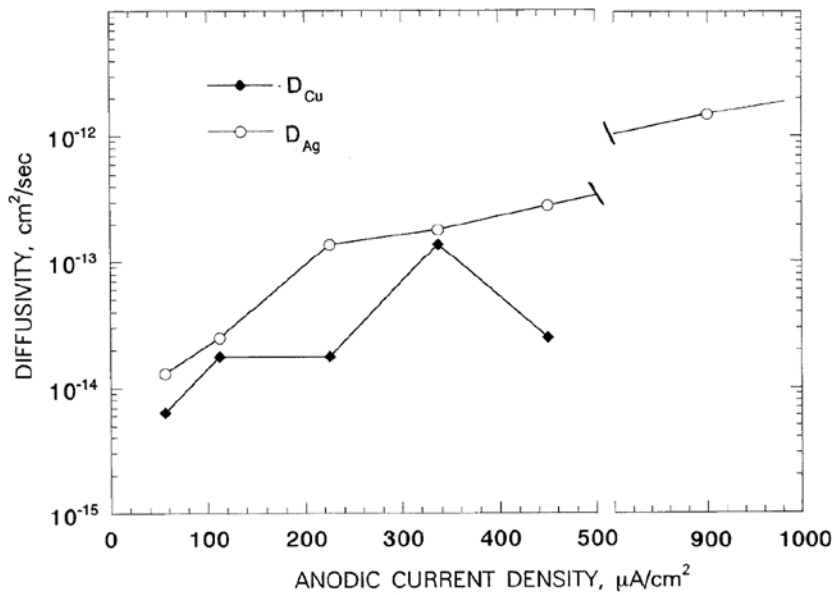


Figure 3-4. Diffusivity of Cu into Ag and Ag into Cu at Cu-Ag interface as a function of anodic current density (current applied to the Cu surface). From Jones et al. (1997).

Jones et al. (1997) propose the following steps for the vacancy movement:

1. Vacancies, V_{Cu} , form by anodic dissolution at the outer Cu surface.
2. V_{Cu} migrate in the outer Cu layer to the Cu-Ag interface. The Cu atoms simultaneously self-diffuse in the opposite direction toward the dissolving surface by exchange with the anodically formed V_{Cu} .
3. Ag vacancies, V_{Ag} , form in the underlying Ag layer by exchange of Ag lattice atoms with V_{Cu} arriving at the Cu-Ag interface. The Ag atoms entering the outer Cu layer further exchange with arriving V_{Cu} , resulting in Ag impurity diffusion in the Cu.
4. V_{Ag} created by step 3 are filled by self-diffusion of Ag, resulting in a flux of Ag atoms within the Ag layer and into the outer Cu layer, accompanied by a flux of V_{Ag} into the Ag layer.
5. Alternative and simultaneous to step 4, Cu atoms jump into all or some of the V_{Ag} created by step 3 at the interface, while the rest move deeper into the Ag by step 4.
6. The Cu impurity diffusion in the Ag occurs by exchange with V_{Ag} previously migrating from the interface in step 4.

Moreover, the presence of hydrogen has been found to increase the vacancy equilibrium concentration in a number of metals (Fukai 2003), which could enhance the Aaltonen-mechanism, i.e. slip-oxidation, by increasing the availability of vacancies at the metal volume ahead of the crack tip. *Ab-initio* calculations performed by Ganchenkova et al. confirmed that in copper, the presence of hydrogen increases the equilibrium vacancy concentration and promotes vacancy clustering and void nucleation (Ganchenkova et al. 2014). Additionally, as in pure copper, vacancy clustering is negligible, due to lack of binding between monovacancies, but in the presence of impurity elements, including S, P and Ag, the formation of divacancies and vacancy clusters is stabilized. The combined effect of both impurities and other species in copper can lead to overcoming the energy barrier for stable vacancy cluster formation and later void nucleation. This increased vacancy equilibrium concentration would then prove to facilitate the Aaltonen, slip-oxidation, mechanism in Cu.

Yagodzinsky et al. (2018) studied the effect of hydrogen on the plastic deformation and free volume generation in oxygen-free copper single crystals. Hydrogen was introduced into the specimens by electrochemical charging in a 0.5M (4.9 %) H_2SO_4 with 20 mg/L $AsNaO_2$ solution⁴ at -350 mV_{SHE} for 69.4 h. It was determined from hydrogen diffusion simulations that this charging resulted in a “rather

⁴ The $AsNaO_2$ acts as a hydrogen recombination poison, in order to enhance/facilitate H uptake by the metal.

homogeneous hydrogen concentration profile” across the specimens. Both charged and uncharged specimens were strained, resulting in remarkably different slip band structures. The formation of free volume (vacancy agglomerates and voids) within the copper was verified using positron annihilation spectroscopy (PAS). Moreover, thermal desorption mass spectroscopy was used to show the hydrogen desorption spectra for as-supplied and hydrogen charged (electrochemical charging using cathodic polarization) conditions. Figure 3-5 shows the desorption spectra for the two material states.

While the large peak at approximately 610 K for the charged state is related to the hydrogen in the lattice (interstitial) sites of the copper after electrochemical charging, the sharp points at low (and very high) temperatures indicate the release of hydrogen from the H-filled voids. In Yagodzinskyy et al. (2018), the deformation mechanism of charged and non-charged single-crystal Cu was also studied. Hydrogen had a clear effect on slip line patterns during straining, with a clear reduction in the distance between slip lines.

Martinsson and Sandström also observed the formation of large void or bubbles in CuOFP. They studied the influence of hydrogen charging method, thermal charging as compared to electrochemical charging, on hydrogen uptake and resulting microstructure in CuOFP in Martinsson et al. (2013) and in Martinsson and Sandström (2012), which focused on electrochemical charging. Thermal charging at 750 °C resulted in significant grain growth and therefore thermal charging was only performed at temperatures up to 675 °C. Previous studies, in which hydrogen was charged thermally, had been performed at higher temperatures, which were not feasible, when aiming to minimize microstructural changes/grain growth. After longer exposures at 600 °C the total hydrogen content of the CuOFP was decreased by approximately 50 %. Their study showed that thermal charging at temperatures in which significant grain growth does not occur of CuOFP does not necessarily increase hydrogen content and therefore this charging method was not considered further (Martinsson et al. 2013).

Electrochemical hydrogen charging was performed in a 10 % H₂SO₄ with 30 mg/L As₂O₃ solution at different current densities for up to three weeks in as-received, annealed and cold worked CuOFP bars and foils of CuOFP. Current density and total charging time had an effect on hydrogen uptake. There was a significant difference between total hydrogen uptake between the bars and foils charged under similar conditions. The origin of this difference was not well understood, but may be attributed to the effect of the larger specific surface area of the foils (Martinsson et al. 2013).

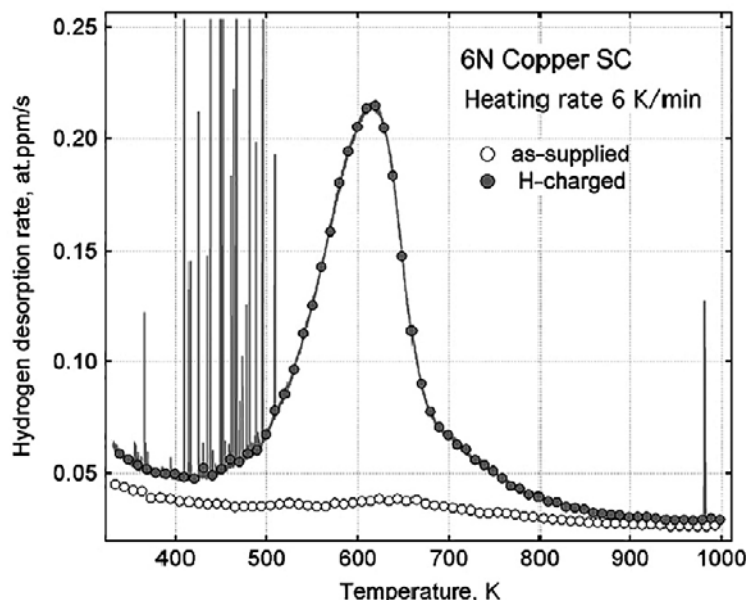


Figure 3-5. Hydrogen desorption from a 6N Copper single crystal (SC) in its as-supplied and electrochemically H-charged states (from Yagodzinskyy et al. 2018). The total H content was 240 at. ppm \approx 4 weight ppm.

Concerning electrochemical charging of the Cu bars, Martinsson and Sandström observe the formation of voids, or "bubbles" as they are referred to by the authors in this publication, as a result of electrochemical charging in Martinsson and Sandström (2012). Most voids were observed within the first 50 μm of the charged surface and preferentially located at or very close to grain boundaries or twins, but smaller bubbles were found intragranularly. The bubbles were estimated to be stable up to approximately 400 MPa. The bubbles' diameter and number density decreased with distance from the surface. A model for hydrogen transport during bubble formation was developed and applied to the experimental H depth profiles, which was in good agreement with experimentally observed parameters. The hydrogen will diffuse across the materials and will accumulate and form hydrogen gas within the bubbles.

Nonetheless, it should be stated that the imposed H-charging conditions, and the use of a recombination poison in the charging solution, creates hydrogen uptake conditions which are more harsh than conditions that the Cu canister will be exposed to in the geological repository. The rapid uptake of hydrogen into the copper specimen could lead to increased vacancy injection, and due to hydrogen's stabilizing effect on vacancy clusters in Cu, the formation, in excess, of voids, which might not be expected in canister exposure conditions.

Another factor that could influence the long-term behaviour of Cu is gamma (γ) radiation, penetrating through the canister wall and interacting with the immediate canister environment, leading to the radiolysis of water and creation of oxidizing and reducing radicals and molecular species, including free electrons, H \cdot , HO \cdot , H₂O₂, etc. In a closed system, the production of radiolysis products would reach steady state in approximately 20 hours, but in repository conditions a closed system cannot be assumed (King et al. 2002). Gamma-radiation induced corrosion in 99.992 % copper (major impurities of Ag and P) in deaerated Millipore MilliQ water was studied by Björkbacka et al. (2012, 2013). The copper cubes were exposed to varying dose rates resulting in accumulated total doses up to 129 kGy⁵. After exposure scanning electron microscope (SEM) investigations revealed that the irradiated specimens were more corroded than the reference state, which was submerged in the same environment, without irradiation (Björkbacka et al. 2012). Additionally, in Björkbacka et al. (2013), a cuprite oxide was identified as the main corrosion product for specimens that accumulated a total dose greater than 20 kGy. The total accumulated dose for the lower and higher dose rates were 62 kGy and 129 kGy. More extensive corrosion was observed on the sample exposed to the higher accumulated, compared to the lower total dose and control specimens, see Figure 3-6 (left). Additionally, Björkbacka et al. (2013) state, that gamma radiation exposure causes enhanced corrosion of copper, and that the "dissolution of copper during irradiation depends on the total absorbed dose." Moreover, they state that "a slight dose rate effect can be observed where a lower dose rate during a longer irradiation time gives a slightly higher amount of dissolved copper than when using a higher dose rate during a shorter irradiation time to reach the same total dose." (Björkbacka et al. 2013). In Hänninen and Yagodzinsky (2017) it is stated that a dose rate of 0.1 Gy/s is approximately 700 times more intense than that at the initial phase of deep repository conditions.

While the role of hydrogen on Cu corrosion was not studied in Björkbacka et al. (2012, 2013), it is known that the radiolysis of water can lead to hydrogen production, and thus a possible source term for hydrogen uptake in a water environment. In Hänninen and Yagodzinsky (2017) and Lousada et al. (2016) corrosion products were also observed on specimens exposed to γ -radiation up to 69 kGy (0.135 Gy/s) and non-irradiated reference specimens exposed in the same water environment, see Figure 3-6 (right). In addition to corrosion products, needle shaped erosion features and islands of needle-shaped crystals were observed on the irradiated specimens (Lousada et al. 2016). Non-irradiated (reference) and γ -irradiated samples were also studied using temperature programmed desorption (TPD) in Hänninen and Yagodzinsky (2017) and Lousada et al. (2016). Resulting TPD spectra and normalized (with respect to the background) desorbed hydrogen and water content measurements are shown in Figure 3-7. More hydrogen is desorbed from the Cu subjected to γ -irradiation (up to 69 kGy at 0.135 Gy/s) as opposed to the non-irradiated (exposed only specimen) and there is an increasing trend in the normalized amount of desorbed hydrogen with increasing total dose.

⁵ In Björkbacka et al. (2012) dose rates of 0.1 (62 kGy total) and 0.21 Gy/s (129 kGy total) were used and in Björkbacka et al. (2013) dose rate of approximately 0.02 Gy/s (0.74 kGy total dose), 0.1 Gy/s (35.4 kGy total dose) and 0.21 Gy/s (74 kGy total dose)

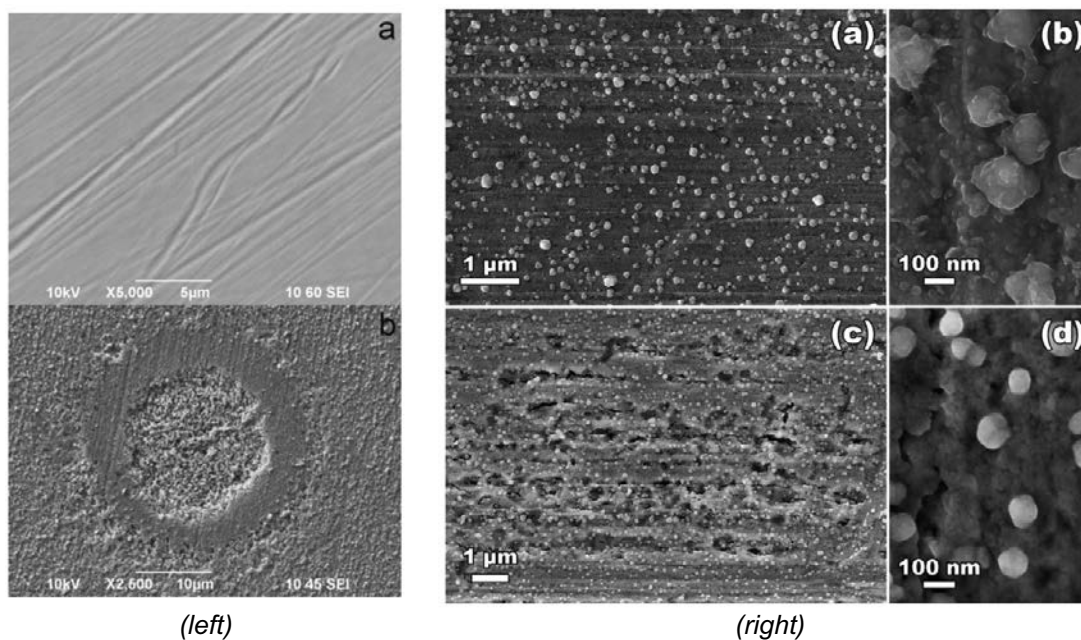


Figure 3-6. (left) SEM images of the surfaces of a (left-a) non-irradiated and (left-b) irradiated Cu-cube from Björkbacka et al. (2012) and (right) SEM images of the surfaces of a (right-a/b) non-irradiated and (right-c/d) irradiated Cu specimen from Lousada et al. (2016).

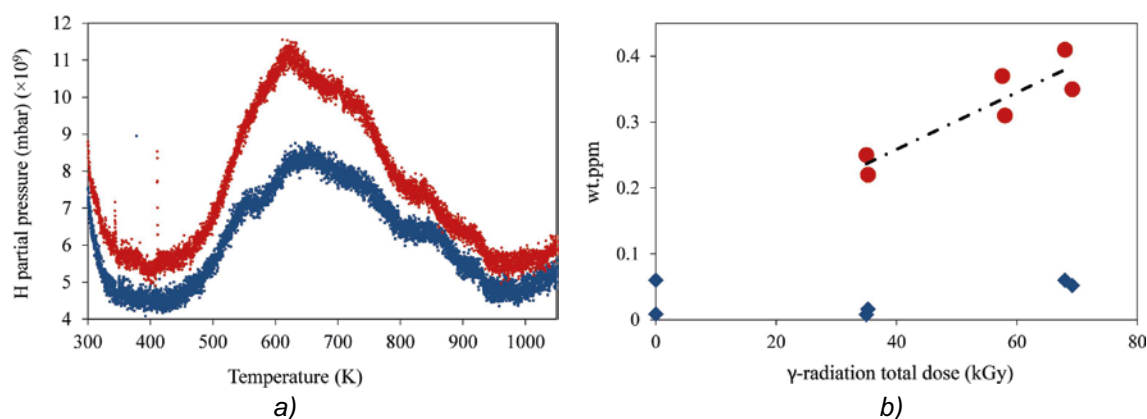


Figure 3-7. (a) H₂ TPD spectra for a non-irradiated copper sample, i.e. background hydrogen content (●), and a γ -irradiated (69 kGy at 0.135 Gy/s) copper sample (●); (b) amount of H₂ (●) and H₂O (◆) measured in samples of copper irradiated up to different total doses in water (the concentrations are normalized with respect to the background) (Lousada et al. 2016).

The studies by Hänninen and Yagodzinskyy (2017) and Lousada et al. (2016) indicate that γ -radiation of copper in an anoxic water environment induces hydrogen uptake with increasing total radiation dose. Nonetheless, as indicated in Hänninen and Yagodzinskyy (2017), the dose rates used in these studies are all greater than 700 times the dose rate that would be expected at the initial phase of the geological repository, thus simulating very harsh environment as compared to realistic exposure conditions and as a result a high total accumulated dose by the material. Based upon these studies, all conducted under conditions that are more harsh than expected in the final repository environment, exposure to irradiation seems to enhance the corrosion of copper. Additionally, hydrogen uptake (hydrogen production during the radiolysis of water) by the material may be observed. The hydrogen could then promote di-vacancy and vacancy cluster stabilization, and the eventual formation of voids, leading to the onset of an Aaltonen mechanism type process.

3.4 Creep as an essential feature in the Aaltonen-mechanism; effect of anodic polarization on creep – results from literature

Aaltonen et al. (2003) measured creep curves using a constant load of 180 MPa on pure copper specimens (0.4×9 mm cross-section and 25 mm gauge length) in 0.3 M NaNO_2 solution at temperatures of $T = 20$ to 80 °C. The specimens were intermittently anodically polarized by a current density of 1 mA/cm^2 in order to see the effect of oxidation/dissolution on the creep rate. They concluded that the (apparent) activation energy for creep (mechanical) was 0.37 eV ($\sim 35 \text{ kJ/mol}$). They observed that the anodic polarization enhanced the creep rate and got an apparent activation energy of 0.2 eV ($\sim 19 \text{ kJ/mol}$) during those stages when the specimens were polarized. The activation energy for the mechanical creep is $\sim 1/4$ of what is given as a lower bound value for Cu at higher temperatures ($T > 413$ °C in Bonora and Esposito (2011)).

The activation energy for the mechanical creep in Aaltonen et al. (2003) is possibly a stress dependent primary stage/transient creep activation energy (although secondary stage steady state creep was claimed). The primary stage creep is associated with microstructural changes (dislocation density changes, arrangement and sub-grain formation while in secondary stage creep the microstructure is in equilibrium (Bonora and Esposito 2011)). This difference may explain the rather low value of the apparent activation energy of mechanical creep proposed by Aaltonen et al. (2003).

Figure 3-8 shows the copper creep result published by Aaltonen et al. (2003). During the initial creep period the specimen was polarised to $E = -100 \text{ mV}_{\text{SCE}}$, which results in the formation of Cu_2O oxide on the surface. The potential of $E = -100 \text{ mV}_{\text{SCE}}$ is close to the open circuit potential (i.e. zero net current density) measured for strained copper specimens (Aaltonen et al. 2003). At about $t = 95$ min the specimen was heavily anodically polarised to a current density of 1 mA/cm^2 (resulting in an increase of the potential to about $E = +100 \text{ mV}_{\text{SCE}}$) and then back to $E = -100 \text{ mV}_{\text{SCE}}$ at about $t = 155$ min. The creep rate shows a clear increase during the heavy anodic polarisation, indicating that the vacancies injected into the specimen during this polarisation period are able to activate dislocation sources. As discussed by Aaltonen et al. (1998), the osmotic stress exerted on dislocations by excess concentration of vacancies can be estimated (Hirth and Lothe 1968) as

$$\sigma = \left(\frac{kT}{V_a} \right) \ln \left(\frac{C_{LV}}{C_{LV}^0} \right) \quad (\text{Equation 3-5})$$

where k – the Boltzmann constant, T – temperature, V_a – atomic volume, C_{LV} and C_{LV}^0 – the vacancy concentrations during polarisation and at equilibrium, respectively. Hirth and Lothe (1968) show that for a vacancy surplus of $C_{LV}/C_{LV}^0 \approx 1.5$ and typical dislocation segment lengths of 0.3 – $0.5 \mu\text{m}$ the osmotic stress reaches the level comparable to the starting stress of Bardeen-Herring dislocation sources.

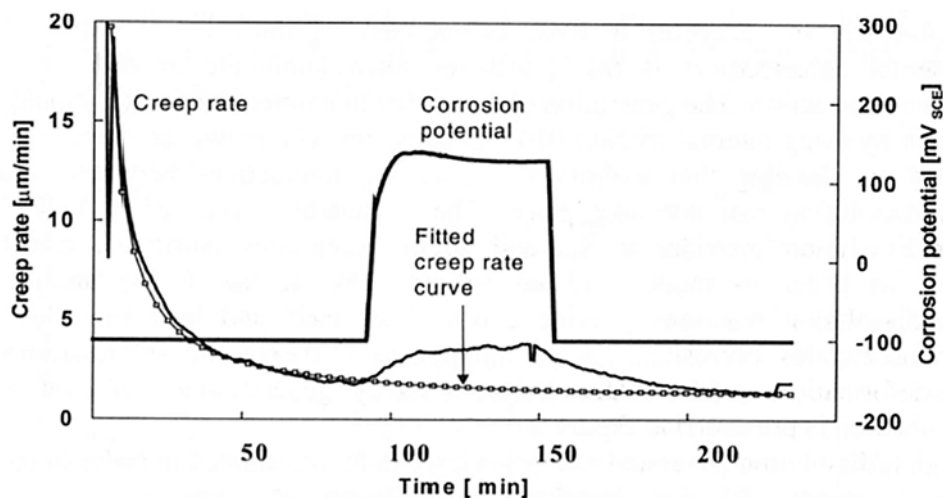


Figure 3-8. Creep rate of cold deformed pure Cu in 0.3 M NaNO_2 solution ($\sigma = 180 \text{ MPa}$, $T = 40$ °C) according to Aaltonen et al. (2003).

After returning the polarisation to $E = -100 \text{ mV}_{\text{SCE}}$, the creep rate returns to the trend line for creep rate at zero net current density within about 60 min time. This is an indication of the time needed for the state of the material to return into its equilibrium condition, i.e. to reach equilibrium concentration of vacancies (or at least of the time needed for the concentration of vacancies to fall below that needed to activate the dislocation sources necessary for the enhanced creep rate to actualise).

According to Aaltonen et al. (1998) and Jagodzinsky et al. (2000), electrochemical oxidation of Cu in 0.3 M NaNO_2 , admiralty brass in tap water, and active dissolution of 5083 Aluminum in KOH solution result in an above thermal equilibrium vacancy concentration and vacancy transport in bulk metal. The existence of the excess vacancies is indicated by peaks in internal friction measurements that are related to dislocations.

Earlier results on the effect of applied potential on creep also exist. Oxide-free copper wires immersed in deaerated acetate buffer of pH = 3.7 at 25 °C were studied by Revie and Uhlig (1974). The authors observed accelerated creep during anodic polarization at a current density of 0.9 mA/cm^2 , Figure 3-9. According to the authors, the data did not support a surface debris layer of high dislocation density, but rather the generation of vacancies by the metal dissolution process during anodic polarisation, and the corresponding reduction of surface energy by cathodic polarization. The Rehbinder effect was proposed as a mechanism for changes in mechanical behaviour during cathodic polarization (i.e. in absence of a surface oxide film).

Surface film formation related vacancy generation or changes in surface free energy resulting in enhanced creep rates have been suspected or shown to take place also in other metals, e.g. in Alloy 600 and nanoporous Au. Andrieu et al. (1998) performed creep tests on Alloy 600 (a nickel-based alloy with a minimum of 72 % Ni) in vacuum and in air at 550 °C. They observed that the creep rates were considerably higher (1–2 orders of magnitude) in air and concluded that the reason could not be the reduction of the specimen geometry due to oxidation or stresses associated with the oxide scale. They also reasoned that the creep mechanism remained the same in both environments (creep power law exponent remained constant) and that the controlling mechanism was interfacial dislocation climb or Bardeen-Herring sources possibly activated by vacancies formed in the oxidation process. The specimens they used were thin, 200 μm , strips. Based on the results of another study by other researchers on thicker Alloy 600 specimens, which did not show any acceleration in air, they concluded that the phenomenon depends on the surface-volume ratio.

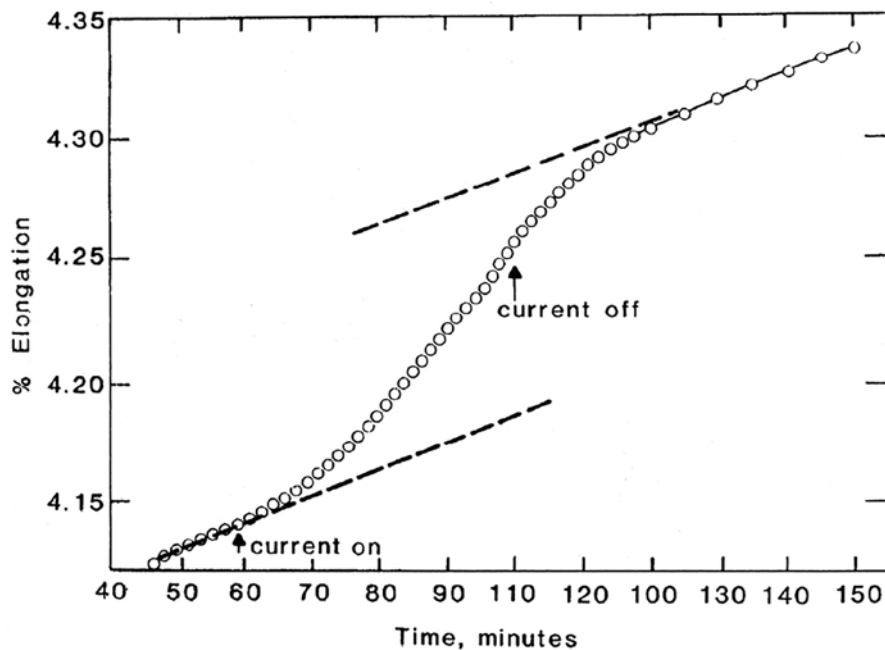
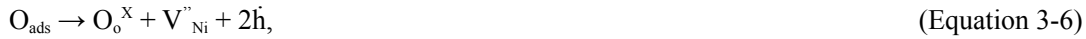


Figure 3-9. Anodically enhanced creep in Cu wire, current density 0.9 mA/cm^2 , equal to a corrosion rate of about 10.4 mm/y . From Jones and Jankovski (1993) (original data published by Revie and Uhlig (1974)).

According to Andrieu et al. (1998), in cationic growing scales, which typically corresponds to the growth of a NiO or Ni-rich oxide scale on Ni-base alloys, the interfacial reactions involved in the growth of a NiO scale are the formation of oxide lattice at the gas-oxide interface



and for the consumption of the metal lattice at the metal-oxide interface



where O_{ads} is an adsorbed oxygen atom, O_o^X is a neutral oxygen in oxide, V''_{Ni} is a vacancy in nickel's place in the oxide with double negative charge, \dot{h} is an electron hole with a positive charge, \underline{Ni}_{alloy} is a nickel atom in the metal lattice, Ni^X_{Ni} is a neutral nickel atom in oxide. In the reactions above, the cation vacancies diffusing towards the oxide-metal interface are annihilated at that interface by the climb of misfit or misorientation interfacial dislocations. The interface acts as a perfect sink for the annihilation of the vacancies and the interface can move freely along with the oxide growth. If the interface cannot move freely, Equation 3-7 changes to



where S denotes vacancy sinks in the alloy. The cation vacancies injected into the alloy diffuse towards internal sinks like grain boundaries, dislocations, etc where they are annihilated. According to Andrieu et al. (1998), if the cation vacancies are not annihilated at the metal-oxide interface, they can be injected into the underlying metal or else can activate the climb of interfacial Bardeen-Herring sources at the metal-oxide interface. Pinning of the oxide-metal interface can take place by heterogeneous oxidation. Increasing temperature would provide an increasing number of sinks resulting in decreasing injection of vacancies and decreasing influence of the oxidation process on the creep rate.

In the Rehbinder (or sometimes Rebinder) effect the plastic behaviour of a material is changed as a consequence of changes in the free surface energy of the material (Mameka 2016). This can be influenced by environment chemistry as well as by polarization as has been demonstrated (Aponete-Roman et al. 2014, Ye and Jin 2014). Effects of polarization on the creep of nanoporous gold with the ligament size of 20 nm in 1 M HClO₄ are shown in Figure 3-10.

Ye and Jin (2013) observed that the creep rate of nanoporous gold increases with potential in the double-layer potential region ($E = 0 V_{SCE}$ to $1.04 V_{SCE}$) while it decreases when oxygen is adsorbed on the surface above the double-layer potential region ($> 1.04 V_{SCE}$). The creep was associated with increased surface diffusivity which was evident by coarsening of the surface layer during polarization. According to Ye and Jin (2013), the probability for a dislocation nucleation and even gliding may increase when the surface atoms become more mobile e.g. because of surface charging.

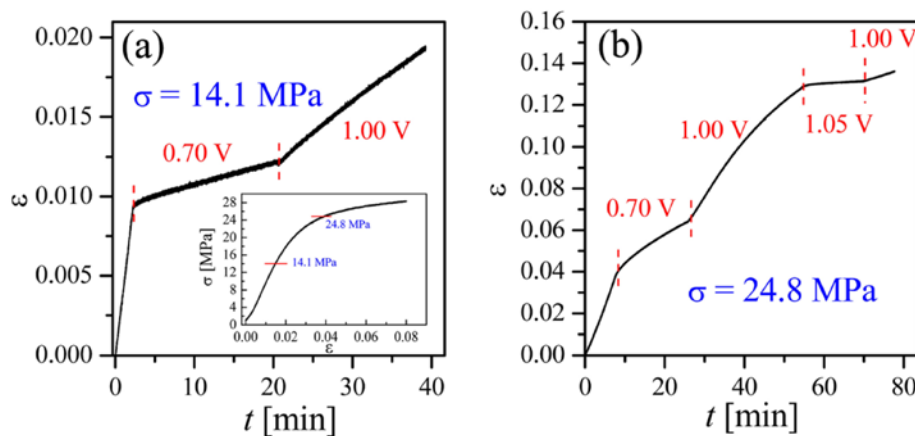


Figure 3-10. Creep of nanoporous gold in 1 M HClO₄ at various polarization potentials under compressive stresses of a) 14.1 and b) 24.8 MPa. The insert in a) shows compression stress-strain curve (Ye and Jin 2013).

Although the Rehbinder effect can explain some polarization effects, the indirect evidences indicate that non-equilibrium vacancy generation at the Cu/Cu₂O interface and diffusion into the copper substrate as divacancies is behind the observed increases in the creep rate in oxidizing conditions. Non-equilibrium vacancies produced in Cu by rapid cooling, cold work, and irradiation anneal out (reach equilibrium) rapidly at room temperature (Jones et al. 1997), so the continued increase in the creep rate requires continuous vacancy generation by Cu atom migration through the film-substrate interface. Based on the creep data shown in Figure 3-8 (Aaltonen et al. 2003) the reaching of near equilibrium vacancy concentration in the Aaltonen et al. case took place in a few tens of minutes after the anodic polarization was finished. On the other hand, the generation of vacancies and their diffusion into the substrate would be supposed to depend on the type of the film and its adherence to the Cu substrate. So far, these data are not known for Cu in sulfide environment.

3.5 Corrosion rate vs current density

The relation between the corrosion rate CR and corrosion current density i_{corr} can be calculated (ASTM 1999) as

$$CR = K_1 \frac{i_{corr}}{\rho} EW \quad (\text{Equation 3-9})$$

where CR is in mm/yr, $K_1 = 3.27 \times 10^{-3} \text{ mm} \times \text{g}/(\mu\text{A} \times \text{cm} \times \text{yr})$, ρ = density (in g/cm³) and EW (a dimensionless unit) = equivalent weight of the corroding metal = W/n , where W = atomic weight and n the number of electrons transferred in the corrosion reaction. In case of copper $\rho = 8.96 \text{ g/cm}^3$ and $EW = 63.54$ for $n = 1$ (Cu⁺) and $EW = 31.77$ for $n = 2$ (Cu²⁺).

Assuming copper is dissolving as a divalent cation, i.e. as Cu²⁺, a current density of $1 \text{ mA/cm}^2 = 1000 \mu\text{A/cm}^2$ used by Aaltonen et al. (1998, 2003) corresponds to a corrosion rate of $CR = 11.6 \text{ mm/yr}$. When comparing this with the average general corrosion rate expected for the repository conditions, i.e. $CR < 1 \text{ mm}/1000.000 \text{ yr} = 10^{-6} \text{ mm/yr}$, it is obvious that the conditions within the experiments performed by Aaltonen et al. are rather extreme. In a recent article King et al. (2017) refer to a copper corrosion current density of $i_{corr} < 10^{-3} \text{ mA/cm}^2$ (i.e. more than $\times 1000$ lower than that used by Aaltonen et al.) from laboratory stagnant conditions for 1.1 mg/l HS^- ($3.32 \times 10^{-5} \text{ mol/l}$) without any transport limitation. King et al. also point out that copper corrosion in repository conditions would be transport limited with about $\times 10^5$ lower transport rate of sulphide than that in the mentioned laboratory experiment. Thus, the general corrosion current density in repository conditions with 1.1 mg/l HS^- would be $i_{corr} < 10^{-8} \text{ mA/cm}^2$, which corresponds to a corrosion rate of about $CR = 10^{-7} \text{ mm/yr}$.

The vacancy generation rate in corrosion is directly related to the corrosion rate and thus to the corrosion current density. Thus, for a very low corrosion rate, such as that expected to prevail in repository conditions with sulphide, the vacancy generation rate is expected to be very low as well. With a low vacancy generation rate, it is probable that the vacancy annihilation rate is comparable or even larger than the generation rate, in which case there would never be an excess of vacancies to diffuse into the material. This assumption is corroborated with the Aaltonen et al. data shown in Figure 3-8, where, after stopping the heavy anodic polarisation, the creep rate is seen to fall back on the reference line within about an hour. This means that at least at the temperature in question, i.e. $T = 40 \text{ }^\circ\text{C}$, the concentration of excess vacancies falls down rapidly after their generation at the surface oxide – solution interface is stopped.

The discussion above with regard to the general corrosion rate is mostly relevant to the possibility of initiating a stress corrosion crack. In case of an already existing and growing stress corrosion crack the situation may be different, since the current density at the tip of a growing crack is typically higher than that of a static surface. This is because at the crack tip, fresh surface (without the protection offered by the surface film) is formed which is in direct contact with the aqueous environment. Yu and Parkins (1987) measured the current density of copper in 1 M NaNO_2 at room temperature, Figure 3-11, in closely similar conditions to those of Aaltonen et al. (1998, 2003). These measurements were performed with straining electrodes, with a very high strain rate of $\dot{\epsilon} = 2 \times 10^{-2} \text{ s}^{-1}$ in order to simulate the advancing crack tip conditions producing fresh bare metal

surface. The values of current density at potential $V = 0.1 V_{SCE}$ were about 100 mA/cm^2 , roughly two orders of magnitude higher than those reported by Aaltonen et al. for the slowly strained and static specimens. The higher current density at the tip of a growing crack would produce a higher concentration of metal vacancies, in terms of the Aaltonen-mechanism. Such straining electrode tests in a relevant sulphidic repository environment have not been made, to the knowledge of the authors of this report. As mentioned above, the current density related to general corrosion of a static copper surface under relevant sulphidic repository conditions is expected to be rather low ($i_{corr} < 10^{-3} \text{ mA/cm}^2$ without and $i_{corr} < 10^{-8} \text{ mA/cm}^2$ with transport limitation). Thus, the current density (and thus also the vacancy generation rate) at the tip of a growing SCC crack (if one could produce such a crack in the first place) under similar conditions would be expected to be much lower than that used by Aaltonen et al. by orders of magnitude.

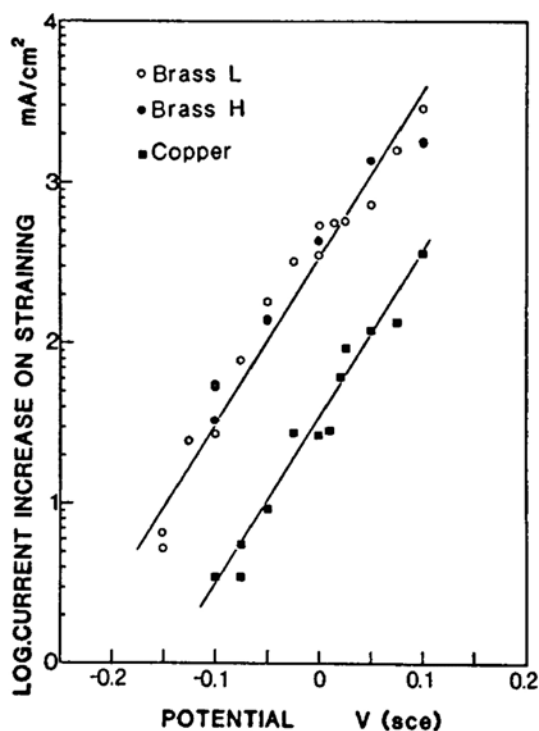


Figure 3-11. Maximum current densities of two brasses and 99.99 % copper in 1.0 M NaNO_2 , pH 9, at room temperature, as a function of potential (V vs SCE). Straining electrodes ($\dot{\epsilon} = 2 \times 10^{-2} \text{ s}^{-1}$) (Yu and Parkins 1987).

4 Conclusions

The so-called Aaltonen-mechanism of SCC was studied in this work. It can be concluded that the said mechanism is actually a refinement of the common slip-oxidation mechanism of SCC, and not a separate new mechanism per se. The Aaltonen-mechanism offers a more detailed hypothesis on what causes the deformation (slip) at the crack tip to localise on certain slip planes, producing high enough strain to break the surface film at the crack tip.

There is ample evidence for vacancies to exist in all metallic materials, including copper, at the concentration of their thermodynamic equilibrium state. A surplus of vacancies can be produced by various external methods, including oxidation (corrosion), resulting in changes in the observed mechanical properties. However, when the external source is removed, the surplus concentration quickly diminishes towards the equilibrium value, with their effect on the mechanical properties diminishing likewise. In one example from Aaltonen et al. (2003), at $T = 40\text{ }^{\circ}\text{C}$, the accelerating effect on creep rate of copper vanished in about one hour from turning off the anodic polarization producing the excessive surplus concentration of vacancies.

Comparing the conditions of generating the excessive surplus concentration of vacancies by anodic oxidation in the Aaltonen et al. experiments to those prevailing in anaerobic sulphidic repository conditions, it is clear that the experimental conditions under which the resulting mechanical property degradation (increase in creep rate) has been observed do not represent any realistic conditions at the repository. Firstly, the environment, highly concentrated NaNO_2 , is never present in the repository. Secondly, copper corrosion in sulphidic environment is different from that in NaNO_2 . Thirdly, the oxidation rate of copper and, thus, the vacancy generation rate in the experiments performed by Aaltonen et al. is higher than that in any realistic sulphidic repository conditions by several orders of magnitude and approaching a factor of $\times 10^6$.

The findings of Taniguchi and Kawasaki (2008), and Becker and Öijerholm (2017) of claimed small (of the maximum depth of tens of microns) SCC cracks on the surface of copper after SSRT experiments can be more convincingly explained as follows: the pre-existing manufacturing defects (which Becker and Öijerholm showed to exist also in unexposed material, that had never been in contact with the sulphide containing environment) extending to the specimen surface, open up due to the effect of surface active sulphide species on the cohesive forces of the opposing surfaces of a defect and can then be erroneously interpreted as cracks (SCC).

Based on the findings of Forsström et al. (2017), the absorbed hydrogen concentration in copper shows no correlation with the sulphide concentration of the environment. Thus, hydrogen can not be responsible to their finding of an increasing number of surface defects (claimed by them to indicate sulphide induced SCC) as a function of increasing sulphide concentration.

5 Summary

The so-called Aaltonen-mechanism of stress corrosion (SCC) cracking has been critically studied in relation to a realistic sulphidic repository environment. The said mechanism is considered to be a refinement of the common slip-oxidation mechanism of SCC, and not a separate new SCC mechanism per se.

While there are ample evidence of excess vacancy generation being able to affect the mechanical properties of metals in different aqueous environments, the data has been gained with very high oxidation rates (current densities corresponding to corrosion rates above 10 mm/y), several orders of magnitude higher than those expected under any realistic repository conditions.

The findings of Taniguchi and Kawasaki (2008), and Becker and Öijerholm (2017) of claimed small (of the maximum depth of a few tens of microns) SCC cracks on the surface of copper after SSRT experiments in sulphide containing environments can be alternatively explained as follows. The pre-existing manufacturing defects (which Becker and Öijerholm showed to exist also in the unexposed material, that had never been in contact with the sulphide containing environment) extending to the specimen surface, open up due to the effect of surface active sulphide species on the cohesive forces of the opposing surfaces of a defect.

Hydrogen ingress into copper as a result of radiation exposure or oxidation reactions at the copper/environment interface is possible, and hydrogen can stabilise vacancies and vacancy clusters in copper. The data from Forsström et al. (2017), however, indicates that hydrogen ingress into copper has no relation to the sulphide concentration of the exposure environment, and thus no relation to the observed shallow (a few tens of micron deep) surface defects.

References

SKB's (Svensk Kärnbränslehantering AB) publications can be found at www.skb.com/publications.

- Aaltonen P, Saario T, Karjalainen-Roikonen P, Piippo J, Tähtinen S, Itäaho M, Hänninen H, 1996.** Vacancy-creep model for EAC of metallic materials in high temperature water. In Proceedings of Corrosion 96, Denver, Colorado, 24–29 March 1996, Paper 81.
- Aaltonen P, Jagodzinski Y, Tarasenko A, Smouk S, Hänninen H, 1998.** Low-frequency internal friction of pure copper after anodic polarisation in sodium nitrite solution. *Corrosion Science* 40, 903–908.
- Aaltonen P, Jagodzinski Y, Hänninen H, 2003.** Vacancy generation in electrochemical oxidation/dissolution of copper in NaNO₂ solution and its role in SCC mechanism: TMS, The Minerals, Metals, and Materials Society. Hydrogen effects on material behavior and corrosion deformation interactions. In Moody N R, Thompson A (eds). Hydrogen effects on material behavior and corrosion deformation interactions: proceedings of the international conference, Jackson Lake Lodge, Wyoming, 22–26 September 2002, 597–606.
- Andrieu E, Pieraggi B, Gourgues A F, 1998.** Role of metal-oxide interfacial reactions on the interactions between oxidation and deformation. *Scripta Materialia* 39, 597–601.
- Aponte-Roman M, Mohanty B, Mann A, 2014.** Chemomechanical effects of self-assembled monolayers on gold films. *Acta Materialia* 68, 52–60.
- Ari-Lahti E, Lehtikuusi T, Olin M, Saario T, Varis P, 2011.** Evidence for internal diffusion of sulphide from groundwater into grain boundaries ahead of crack tip in Cu OFP copper. *Corrosion Engineering, Science and Technology* 46, 134–137.
- ASTM, 1999.** ASTM G102-89: Standard practice for calculation of corrosion rates and related information from electrochemical measurements. West Conshohocken, PA: ASTM International.
- Bhaskaran G, Carcea A, Ulaganathan J, Wang S, Huang Y, Newman R C, 2013.** Fundamental aspects of stress corrosion cracking of copper relevant to the Swedish deep geologic repository concept. SKB TR-12-06, Svensk Kärnbränslehantering AB.
- Becker R, Öijerholm J, 2017.** Slow strain rate testing of copper in sulfide rich chloride containing deoxygenated water at 90 °C. SSM report 2017:2, Swedish Radiation Safety Authority.
- Björkbacka Å, Hosseinpour S, Leygraf C, Jonsson M, 2012.** Radiation induced corrosion of copper in anoxic aqueous solution. *Electrochemical and Solid-State Letters* 15, C5–C7.
- Björkbacka Å, Hosseinpour S, Johnson M, Leygraf C, Jonsson M, 2013.** Radiation induced corrosion of copper for spent nuclear fuel storage. *Radiation Physics and Chemistry* 92, 80–86.
- Björkblad A, Faleskog J, 2018.** Evaluation of Cu-OFP creep crack growth and theoretical fracture models for Cu-OFP. Posiva SKB Report 03, Posiva Oy, Svensk Kärnbränslehantering AB.
- Bonora N, Esposito L, 2011.** Transient creep modeling based on the dependence of the activation energy on the internal stress. In Proceedings of Convegno Nazionale IGF XXI, Cassino, Italy, 13–15 June 2011, 120–125.
- Bourassa R R, Lengeler B, 1976.** The formation and migration energies of vacancies in quenched copper. *Journal of Physics F: Metal Physics* 6, 1405. doi: 10.1088/0305-4608/6/8/003
- Caskey G R, Dexter A H, Holzworth M L, Louthan M R, Derrick R G, 1975.** Hydrogen transport in copper. Presented at Materials Science Symposium of AIME, Cincinnati, Ohio, 11-13 November 1975. Available at: <https://digital.library.unt.edu/ark:/67531/metadc721542/>
- Forsström A, Becker R, Öijerholm J, Jagodzinski Y, Hänninen H, Linder J, 2017.** Hydrogen absorption in copper as a result of corrosion reactions in sulphide and chloride containing deoxygenated water at 90 °C in simulated spent nuclear fuel repository conditions. In Proceedings of the EUROCORR 2017 & 20th International Corrosion Congress ICC, Prague, 3–7 September 2017.

- Fukai Y, 2003.** Superabundant vacancies formed in metal–hydrogen alloys. *Physical Scripta* T103, 11–14.
- Ganchenkova M G, Yagodzinskyy Y N, Borodin V A, Hänninen H, 2014.** Effects of hydrogen and impurities on void nucleation in copper: simulation point of view. *Philosophical Magazine* 94, 3522–3548.
- Hirth J, Lothe J, 1968.** *Theory of dislocations*. New York: McGraw-Hill.
- Hänninen H, Yagodzinskyy Y, 2017.** Hydrogen absorption and behavior in copper as a result of corrosion reactions and γ -radiation in spent nuclear fuel repository conditions. Presentation from Finnish Research Programme on Nuclear Waste Management (KYT) 2015–2018, Aalto University, Espoo, Finland, 15 December 2016. Available at: http://kyt2018.vtt.fi/copper_corrosion/Hanninen.pdf
- Jagodzinski Y, Aaltonen P, Smouk S, Tarasenko A, Hänninen H, 2000.** Internal friction study of environmental effects on metals and alloys. *Journal of Alloys and Compounds* 310, 256–260.
- Jones D, Jankowski A, 1993.** Anodically enhanced creep in Cu/Ag thin film couples. Presented at Alloy 600 PWSCC Experts Meeting, Arlie, Virginia, 6–9 April 1993. Available at: https://inis.iaea.org/collection/NCLCollectionStore/_Public/26/058/26058570.pdf
- Jones D A, Jankowski A F, Davidson G A, 1997.** Room-temperature diffusion in Cu/Ag thin-film couples caused by anodic dissolution. *Metallurgical and Materials Transactions A* 28, 843–850.
- Jones R H (ed), 1992.** *Stress-corrosion cracking*. Materials Park, OH: ASM International.
- King F, Newman R, 2010.** Stress corrosion cracking of copper canisters. SKB TR-10-04, Svensk Kärnbränslehantering AB.
- King F, Ahonen L, Taxén C, Vorinen U, Werme L, 2002.** Copper corrosion under expected conditions in a deep geologic repository. Posiva 2002-01, Posiva Oy, Finland.
- King F, Chen J, Qin Z, Shoemith D, Lilja C, 2017.** Sulphide-transport control of the corrosion of copper canisters. *Corrosion Engineering, Science and Technology* 52, 210–216.
- Lousada C M, Soroka I L, Yagodzinskyy Y, Tarakina N V, Todoshenko O, Hänninen H, Korzhavyi P A, Jonsson M, 2016.** Gamma radiation induces hydrogen absorption by copper in water. *Nature Scientific Reports* 6, 24234. doi:10.1038/srep24234
- Lejček P, 2010.** *Grain boundary segregation in metals*. Berlin, Heidelberg: Springer.
- Magnusson H, Frisk K, 2013.** Self-diffusion and impurity diffusion of hydrogen, oxygen, sulphur and phosphorus in copper. SKB TR-13-24, Svensk Kärnbränslehantering AB.
- Mameka N M, 2016.** Surface-controlled mechanical properties of bulk nanoporous gold. PhD thesis. *Werkstoffphysik und -technologie M-22*, Technische Universität Hamburg.
- Martinsson Å, Sandström R, 2012.** Hydrogen depth profile in phosphorus-doped oxygen-free copper after cathodic charging. *Journal of Materials Science* 47, 6768–6776.
- Martinsson Å, Sandström R, Lilja C, 2013.** Hydrogen in oxygen-free, phosphorus-doped copper: charging techniques, hydrogen contents and modelling of hydrogen diffusion and depth profile. SKB TR-13-09, Svensk Kärnbränslehantering AB.
- Mattsson E, Schueckher F, 1958.** An investigation of hydrogen embrittlement in copper. *Journal of the Institute of Metals* 87, 241–247.
- Revie R, Uhlig H, 1974.** Effect of applied potential and surface dissolution on the creep behavior of copper. *Acta Metallurgica* 22, 619–627.
- San March C, Somerday B P, 2012.** Technical reference for hydrogen compatibility of materials. SAND2012-7321, Sandia National Laboratories.
- Sipilä K, Arilahti E, Lehtikuusi T, Saario T, 2014.** Effect of sulfide exposure on mechanical properties of CuOFP. *Corrosion Engineering, Science and Technology* 49, 410–414.
- Taniguchi N, Kawasaki M, 2008.** Influence of sulfide concentration on the corrosion behavior of pure copper in synthetic seawater. *Journal of Nuclear Materials* 379, 154–161.

Taxén C, Flyg J, Bergqvist H, 2018. Stress corrosion testing of copper in sulfide solutions. SKB TR-17-16, Svensk Kärnbränslehantering AB.

Yagodzinskyy Y, Malitckii E, Tuomisto F, Hänninen H, 2018. Hydrogen-induced strain localization in oxygen-free copper in the initial stage of plastic deformation. Philosophical Magazine 98, 727–740.

Ye X-L, Jin H-J, 2013. Electrochemical control of creep in nanoporous gold. Applied Physics Letters 103, 201912. doi:10.1063/1.4831686

Yu J, Parkins R N, 1987. Stress corrosion crack propagation in α -brass and copper exposed to sodium nitrite solutions. Corrosion Science 27, 159–182.

SKB is responsible for managing spent nuclear fuel and radioactive waste produced by the Swedish nuclear power plants such that man and the environment are protected in the near and distant future.

skb.se